Polymer Degradation and Stability 134 (2016) 186–193

Contents lists available at ScienceDirect

Polymer Degradation and Stability

journal homepage: www.elsevier.com/locate/polydegstab

Flame retardancy of phosphorus-containing ionic liquid based epoxy networks

Rodolphe Sonnier [a, *], Loïc Dumazert [a], Sébastien Livi [b], Thi Khanh Ly Nguyen [b], Jannick Duchet-Rumeau [b], Henri Vahabi [c], Pascal Laheurte [d]

[a] Ecole des Mines d'Alès, Centre des Matériaux des Mines d'Alès – Pôle Matériaux Polymères Avancés, 6 Avenue de Clavières, 30319, Alès Cedex, France
[b] Université de Lyon, F-69003, Lyon, France; INSA Lyon, F-69621, Villeurbanne, France; CNRS, UMR 5223, Ingénierie des Matériaux Polymères, France
[c] Université de Lorraine, Laboratoire MOPS E.A. 4423, Metz, F-57070, France
[d] Université de Lorraine, Laboratoire LEM3 UMR 7239, Metz, F-57045, France

ARTICLE INFO

Article history:
Received 1 July 2016
Received in revised form
7 October 2016
Accepted 14 October 2016
Available online 15 October 2016

Keywords:
Ionic liquid
Epoxy networks
Flame retardancy
Phosphorus flame retardant

ABSTRACT

Various amounts of a phosphonium ionic liquid (IL169) were used as curing agents as well as flame retardants of epoxy prepolymer in order to prepare epoxy networks with improved fire properties. The flame retardancy of these resins was investigated using thermogravimetric analysis (TGA), pyrolysis-combustion flow calorimetry (PCFC) and cone calorimetry. Phosphonium ionic liquid significantly reduced flammability without further addition of flame retardants due to the high amount of phosphorus (up to 3.69 wt%). The Peak of heat release rate decreases from 1099 kW/m^2 to 300 kW/m^2 in cone calorimeter at 35 kW/m^2 when incorporating 30 phr of IL169. Phosphorus modifies pyrolysis pathway, promotes charring and may act as flame inhibitor. The char layer protects the underlying polymer, leading to a high unburnt polymeric fraction. Char properties were studied using PCFC, Raman spectroscopy and X-ray tomography. Phosphorus improved the graphitization of the char and its thermo-oxidative stability.

1. Introduction

Epoxy resins are widely used in many applications, including composite and coating industries. They are among the highest flammable thermosets together with unsaturated polyesters. Thus, many efforts have been made to improve the flame retardancy of these resins in order to extend their applications [1]. Phosphorus-based additives have been used as alternatives to halogen-based flame retardants (FRs) while some of the latter were banned due to environmental concerns [1–4]. Phosphorus-based epoxy monomers or curing agents have also been investigated as flame retardants [5–10]. Indeed, the reactive approach seems to be slightly more efficient, allows maintaining transparency, and is believed to suppress possible migration of flame retardants over time [11–12]. More recently, biobased additives or reactive hardeners have been developed [11,13] and some fully biobased and flame retarded epoxy resins have been synthetized [14].

According to the literature, phosphate and phosphonate-based FRs act mainly in condensed phase by promoting charring of the epoxy resin [5–6]. Intumescent mono-component solutions led to a significant reduction of flammability. Phosphorus compounds decompose into phosphoric acids resulting in the dehydration of the epoxy resin which is necessary for promoting charring. However, the presence of phosphorus compounds could also reduce the thermal stability of the resin. Phosphinate and phosphine oxide-based FRs may be more active in gas phase, decreasing the combustion efficiency. The extent of flame retardancy depends primarily on the phosphorus content (typically higher than 1 wt%).

Ionic liquid (IL)-based epoxy resins are a new class of epoxy thermosets [15]. According to the literature, Livi et al. have demonstrated that the basicity of the ionic liquids (phosphinate, phosphate or dicyanamide) initiates the epoxy polymerization and binds covalently to the network through an anionic polymerization. These new curing agents of epoxy prepolymer lead to networks with enhanced final properties such as an excellent thermal stability, higher hydrophobic behavior and good thermo-mechanical properties [16–20]. Thanks to the great diversity of IL, properties can be finely tuned [21]. The thermal stability and flammability of ILs have already been studied, and vary to a great extent depending

* Corresponding author.
E-mail address: rodolphe.sonnier@mines-ales.fr (R. Sonnier).

http://dx.doi.org/10.1016/j.polymdegradstab.2016.10.009
0141-3910/

on their nature [22–23]. While some ionic liquids contain phosphorus groups, low-flammability epoxy resins can be expected without further addition of flame retardants.

The objective of this article is to assess the flame retardancy of epoxy resins crosslinked with various amounts of a phosphorus-based ionic liquid (namely IL169). The modes-of-action of phosphorus were identified and the properties of the char formed during burning were investigated in detail.

2. Experimental

2.1. Materials

Diglycidyl ether of bisphenol A (DGEBA) based epoxy prepolymer (DER 332) with an epoxide equivalent weight (EEW) of 175 g mol^{-1} was purchased from DOW Chemical Company. Jeffamine D230 was supplied by Huntsman and was used as conventional curing agent. Phosphonium ionic liquid: Tributyl(ethyl) phosphonium diethyl-phosphate named IL169 was kindly provided by Cytec, Inc. All the chemical structures are shown in Fig. 1.

To prepare samples, DGEBA and curing agents (i.e. Jeffamine D230 and IL169) were mixed with a suitable ratio under stirring at room temperature for 30 min. The mixture was then degassed in an ultrasonic bath for 15 min, and was poured into silicone molds prior to curing. The ratio between DGEBA and curing agents as well as the curing and post-curing conditions are presented in Table 1.

2.2. Differential scanning calorimetry

Differential Scanning Calorimetry thermograms (DSC) of epoxy/amine and epoxy/IL networks were recorded using a DSC Q20 TA instruments from 20 to 250 °C during heating at a rate of 10 K min^{-1} under nitrogen flow of 50 mL min^{-1}.

2.3. Thermogravimetric analysis

Thermogravimetric analyses (TGA) were performed using a Setsys Evolution apparatus (Setaram). 10 (±2) mg-samples were heated under nitrogen flow (100 mL/min) at a heating rate equal to 10 °C/min from room temperature to 900 °C.

2.4. Pyrolysis-combustion flow calorimeter

Flammability was investigated using a pyrolysis combustion flow calorimeter (PCFC) which was developed by Lyon and Walters [24]. The sample (3 ± 1 mg) was first heated from 80 to 750 °C at 1 °C/s in a pyrolyzer under nitrogen flow and the degradation products were sent to a combustor where they were mixed with oxygen in excess at 900 °C. In such conditions, these products were fully oxidized. The heat release rate (HRR) was then calculated by oxygen depletion according to Huggett's relation (1 kg of consumed oxygen corresponds to 13.1 MJ of released energy) [25]. All materials were tested twice at least. The variation in main data (peak of heat release rate, total heat release and heat of complete combustion) was lower than 10% and the variation in the temperature of pHRR was around 10 °C.

The thermo-oxidative stability of residues from cone calorimeter was also studied in PCFC according to method B, i.e. in aerobic pyrolysis, for various oxygen fractions in pyrolysis chamber (from 0.01 to 0.4) as proposed elsewhere [26]. The temperature of char degradation is the temperature at which the HRR reaches 50 W/g.

2.5. Cone calorimeter

Some flame retardant effects (as barrier effect or flame inhibition) are not effective in PCFC. Therefore fire behavior was also studied using a cone calorimeter (Fire Testing Technology) which is a powerful tool to investigate the fire behavior of polymers. A horizontal sample sheet of 100 × 100 × 3 mm^3 was placed at 2.5 cm below a conic heater and isolated by rock wool. The samples were exposed to 35 kW/m^2 in well-ventilated conditions (air rate 24 L/s) in the presence of a spark igniter to force the ignition. HRR was determined according to oxygen depletion (Huggett's relation) as in PCFC. This test was performed according to the ISO 5660 standard. All materials were tested twice with a good repeatability. The variation on main data (time-to-ignition, peak of heat release rate, total heat release, smoke extinction area, residue content and effective heat of combustion) was lower than 10% except for pHRR of 10IL and the char content was 20IL (15–20% of variation).

2.6. Raman spectroscopy

Raman spectra were carried out to study the graphitization of the chars. Spectra were measured using a Horiba Jobin Yvon LabRAM Aramis spectrophotometer fitted with a 532 nm laser and a 200 μm confocal pinhole. The laser was focused using a × 10 objective. All spectra were obtained with an integration time of 30 s accumulation of 4 spectra recorded in the spectral range 800–1900 cm^{-1}.

2.7. X-ray tomography analyses

X-ray tomography is a powerful tool to assess the morphology of the char [27–29]. To obtain 3D visualization of the inner residues, a fraction of 30 × 30 × 30 mm^3 of the residue collected from cone calorimeter test was analyzed using non-destructive Analysis X-ray micro-tomography EasyTom with a LaB6 filament and a flat panel with a resolution of 2320 × 2336. The volume of material is 30 × 30 × 30 mm^3 with a resolution of 34 microns. The volume reconstruction was obtained from a set of 1900 slices obtained after 1800 rotations. The diagram of the analysis is shown in Fig. 2.

2.8. Scanning electron microscopy coupled with Energy Dispersive X-ray spectroscopy (SEM-EDX)

Chars were observed using a FEI Quanta 200 scanning electron microscope and char composition (C, O, P atoms) was determined by Energy Dispersive X-ray spectroscopy (EDX) using Oxford INCA Energy 300 system and a detector of 133 eV (at Mn). For each char, the composition of at least three zones was analyzed. Note that hydrogen content cannot be measured using SEM-EDX.

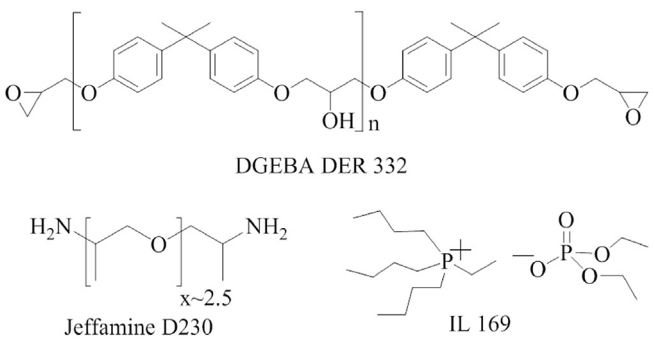

Fig. 1. Chemical structures used in this study.

Table 1
Formulations studied in this article.

Formulation	Glass transition temperature (°C)	Curing agent	Curing agent part (phr)	Curing conditions	Post-curing conditions	Phosphorus content (wt%)
0IL	90	D230	34	2 h at 80 °C, 3 h at 125 °C	1 h at 200 °C	0
10IL	114	IL169	10	2 h at 80 °C, 3 h at 160 °C	3 h at 200 °C	1.45
20IL	108	IL169	20	2 h at 80 °C, 3 h at 160 °C	3 h at 200 °C	2.67
30IL	93	IL169	30	2 h at 80 °C, 3 h at 160 °C	3 h at 200 °C	3.69

3. Results and discussion

3.1. Micro-scale behavior

Thermogravimetric (TG) and differential thermogravimetric (DTG) curves are shown in Fig. 3 for all samples. The main data are summarized in Table 2. The phosphorus-free resin is decomposed in one step starting at 300 °C and leaving a small residue. The incorporation of phosphorus reduces only slightly the thermal stability (measured using the temperature for 5% of mass loss $T_{5\%}$). The peak of mass loss rate decreases and its temperature increases by a few degrees. A shoulder is observed at higher temperatures (close to 400 °C). For 30IL, a second shoulder is also noted above 450 °C. The residue content is higher (around 20 wt%) than for 0IL (10.4 wt%). Its value is stable whichever the phosphorus content. Around 400 °C, the discrepancy between the residue contents for 0IL and for phosphorus-based epoxy resins is higher: 21 wt% and 40–42 wt% respectively.

Heat release rate curves from PCFC tests are shown in Fig. 4. The main data from these tests can be found in Table 2. Even if the heating rate is higher than in TGA (60 °C/min versus 10 °C/min), the curve profiles are similar in both tests. The decomposition occurs through one main step but shoulders can be observed at high temperature, particularly for 30IL. Phosphorus slightly reduces the thermal stability (the heat release starts at lower temperature than for 0IL) but the temperature of the peak T_{pHRR} is slightly higher (382–391 versus 374 °C for 0IL). The peak of heat release rate, related to the peak of mass loss rate in TGA, decreases linearly with the phosphorus content (see Fig. 5). Such a relation was already observed for epoxy resins flame retarded with phosphorus-containing additives [11,13]. Total heat release (THR) is lower for phosphorus-containing resins (22.6–23.9 kJ/g versus 26.5 kJ/g for 0IL). Char contents are slightly lower in PCFC than in TGA. As noted by Müller et al. [28], this difference is due to the higher heating rate in PCFC. Nevertheless in both cases, the char content for IL-containing resins is more or less constant and slightly higher than for 0IL. The heat of complete combustion of the volatiles ($h_{c,gas}$) is calculated as the THR in PCFC divided by the mass loss. The heat of complete combustion of volatiles is similar for all epoxy resins (around 27–28 kJ/g).

On the whole, the incorporation of phosphorus from ionic liquid IL169 allows to reduce the peak of heat release rate and to moderately increase the residue content without lowering the thermal stability, which is quite often observed when phosphorus flame retardants are added. The reduction in pHRR with increasing phosphorus content can be attributed to a change in the thermal decomposition mechanism that results in less heat being released over a broader temperature range. While some flame retardant effects are not available at microscale, cone calorimeter tests were also performed.

3.2. Cone calorimeter results (bench scale)

Fig. 6 shows the heat release rate curves for all materials studied in cone calorimeter at 35 kW/m^2. Table 3 summarizes the main data. The phosphorus-free epoxy resin (0IL) presents a very high peak of heat release rate (pHRR) (higher than 1000 kW/m^2). The residue content is very small and the combustion is almost complete. The increase in phosphorus content allows for a significant reduction of the pHRR to 300 kW/m^2 (- 73% for 30IL). The residue content increases up to 39 wt% for 30IL. The effective heat of combustion is lowered (19.1–21.6 kJ/g versus 24.3 kJ/g). Consequently the total heat release is divided by almost 2 (from 23.7 kJ/g for 0IL to 12.7 kJ/g for 30IL). Interestingly, the time-to-ignition remains stable around 100s for all resins. This is not common, as many phosphorus flame retardants promote fast ignition due to a loss in thermal stability. This is in agreement with TG and PCFC analyses: thermal stability is similar whatever the IL169 content.

Fig. 7 shows the residues sampled from cone calorimeter tests. It can be observed that the residues from epoxy resins containing ionic liquid IL169 are expanded. The higher the IL169 content, the higher the expansion is during the test. Movie M1 (see supporting information) shows the development of the expanded residue for 30IL. The intumescence starts after ignition and continues throughout the test. Nevertheless, the expansion is quite slow, in comparison to other flame retarded epoxy resins [11]. The rate of char formation and expansion needs further investigation.

3.3. Modes-of-action of phosphorus

Phosphorus can act by modifying pyrolysis mechanisms but also by flame inhibition or barrier effect. These various modes-of-action need to be assessed.

Flame inhibition may be assessed using different parameters, including smoke production rate, combustion efficiency and CO/CO_2 ratio. Usually, combustion efficiency is calculated as the effective heat of combustion in cone calorimeter divided by the

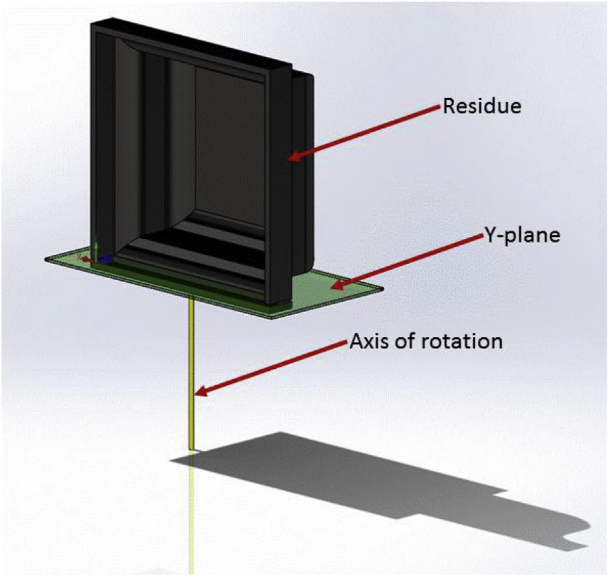

Fig. 2. Diagram of X-ray tomography analysis.

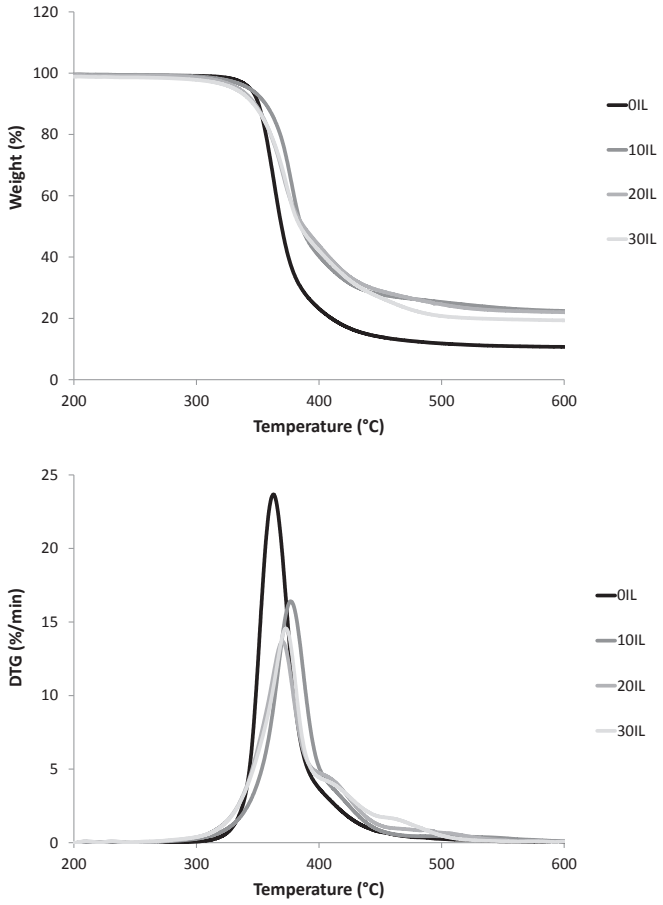

Fig. 3. TG (top) and DTG (bottom) curves for studied epoxy resins (under nitrogen flow).

heat of complete combustion of the volatiles ($h_{c,gas}$). Nevertheless, in our case, the calculation is questionable, particularly for 30IL because the mass loss is not the same at microscale and at bench scale. However for 0IL and 10IL the char content is similar in both tests. It can be noted that the combustion efficiency is much lower for 10IL: 0.71 versus 0.87 for 0IL.

CO/CO_2 ratio curves during cone calorimeter test are shown in Fig. 8. It can be noted that this ratio increases with the IL169 content during burning (100–400 s). The mean value for 30IL is six times the value for 0IL (0.12 versus 0.02). A fast increase in the CO/CO_2 ratio is observed at the end of the test when the flame starts to vanish (the temperature in the combustion zone decreases). Table 3 shows the Smoke Extinction Area (SEA), which represents the effective optical obscuring area generated by 1 kg of mass loss. This parameter depends on the combustion efficiency but also on the degradation rate. SEA is the lowest for the phosphorus-free epoxy resin despite a much higher heat release rate. These observations are not final evidence of a flame inhibition effect provided by IL169,

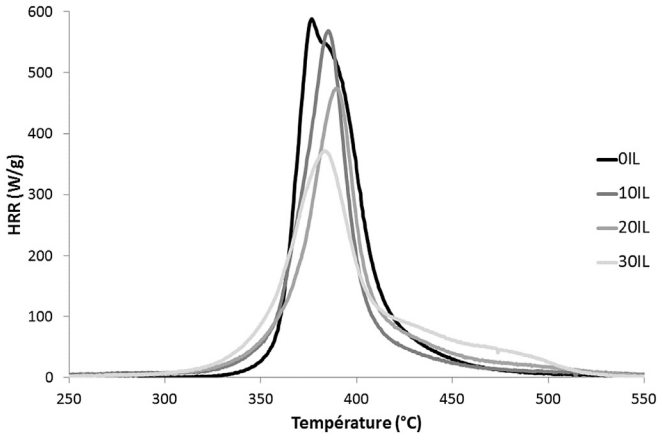

Fig. 4. Heat release rate curves for epoxy resins in PCFC test.

but are in agreement with such an assumption.

Fig. 9 presents the residue content in cone calorimeter and the difference between the residue contents in cone calorimeter and in PCFC as a function of phosphorous content in the resin. The residue content in PCFC is lower for 0IL sample (5.5 wt%) than for IL-containing resins but stable for phosphorus-containing epoxy resins (14.5–16 wt%). On the contrary, the residue content in cone calorimeter linearly increases when IL169 content increases. Müller et al. have shown that the char content from epoxy resins is dependent on the heating rate [28]. This may explain the slight difference observed between the char contents in cone calorimeter and in PCFC for 0IL and 10IL. On the contrary, a significant gap is observed for 20IL and 30IL. The barrier effect provided by the expanded char in cone calorimeter test is very efficient for 20IL and 30IL. Then a fraction of the underlying polymer is not fully decomposed leading to an increase in the residue content. In this case, the residue is not composed of char only, but also of non-pyrolyzed polymer. The very high amount of residue for 30IL is a convincing indication evidencing the role of the expanded char as barrier layer.

3.4. Study of chars

Table 4 shows the elemental composition of the chars sampled from cone calorimeter tests. The residues obtained at the end of cone calorimeter test were picked up in the core of char under a protective top layer for 10, 20 and 30IL. Therefore, they do not correspond to the fraction of non-pyrolyzed resin located at the bottom of the residue. On the contrary, any cohesive layer is formed on the whole surface during burning for 0IL. This sample collected is hardly comparable to that of phosphorus-containing resins. Its composition is very different from the other ones, with a very high content of carbon even if this sample was not protected from heat and oxygen by a top layer at the end of the test (when thermo-oxidation may occur).

Table 2
Main data from thermogravimetric analyses and PCFC tests.

Formulation	P content (wt%)	TGA			PCFC				
		$T_{5\%}$ (°C)	T_{peak} (°C)	Residue at 700 °C (wt%)	pHRR (W/g)	T_{pHRR} (°C)	THR (kJ/g)	Residue at 750 °C (wt%)	$h_{c,gas}$ (kJ/g)
0IL	0	344	363	10.4	555	374	26.5	5.5	27.9
10IL	1.45	343	377	21.5	506	382	22.6	15.5	26.8
20IL	2.67	334	374	21.1	470	391	22.9	16	27.3
30IL	3.69	331	369	18.6	388	383	23.9	14.5	27.9

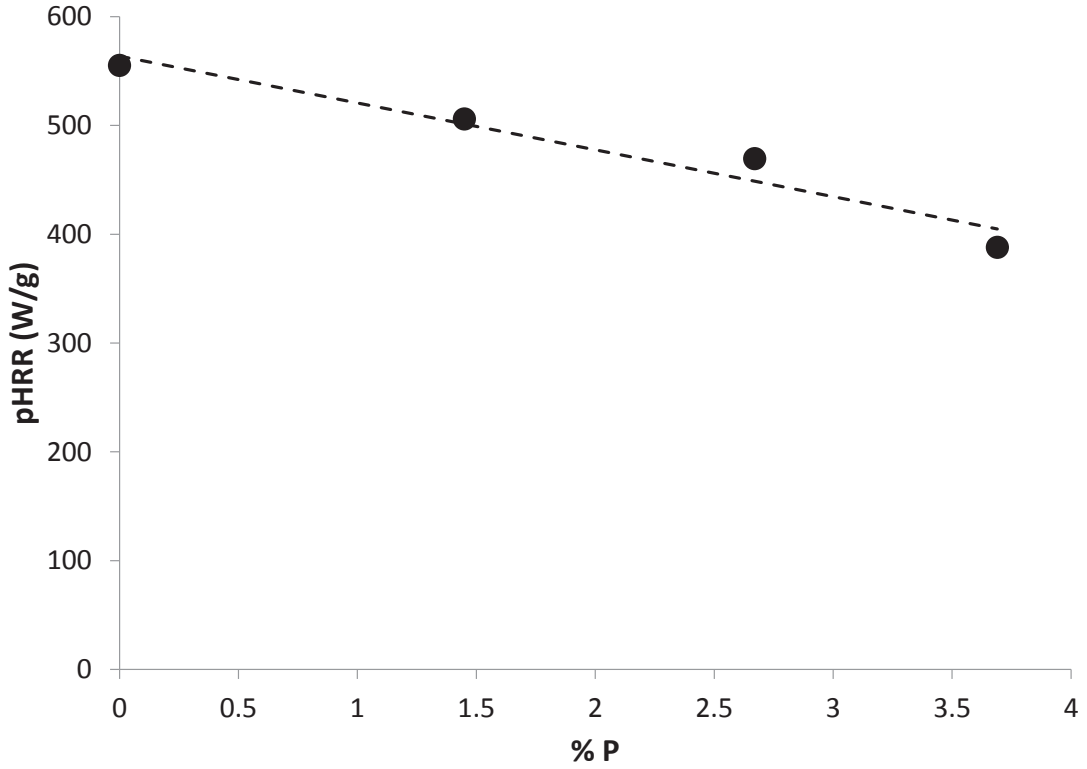

Fig. 5. Peak of heat release rate in PCFC test versus phosphorus content in epoxy networks.

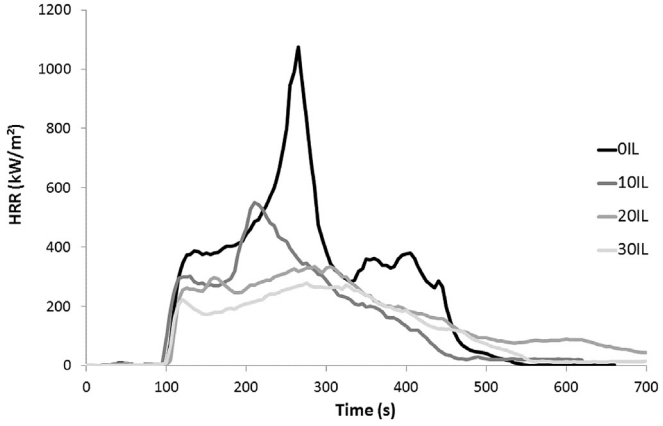

Fig. 6. Heat release rate curves for epoxy cured with amine (D230) and ionic liquid (IL169) in cone calorimeter test (heat flux 35 kW/m^2).

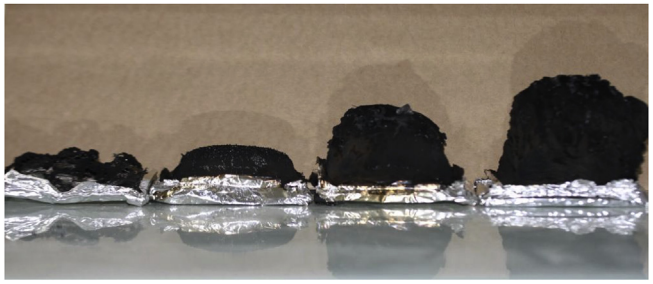

Fig. 7. Residues after cone calorimeter tests (from left to right: 0IL, 10IL, 20IL, 30IL).

The composition of chars from phosphorus-containing resins is quite similar but the content in carbon tends to decrease from 71.6 wt% for 10IL to 65.4 wt% for 30IL. On the contrary, the oxygen and phosphorus contents tend to increase.

Phosphorus contents in residues from PCFC and cone calorimeter tests are plotted versus the initial phosphorus contents in epoxy resins in Fig. 10. The phosphorus content in residues, from PCFC or cone calorimeter, increases linearly with the initial phosphorus content in resin. Moreover PCFC and cone calorimeter tests lead to similar phosphorus contents in residues considering standard deviations.

Considering the phosphorus contents in PCFC residue and in epoxy resin and the mass loss in PCFC analysis, it is possible to calculate the amount of phosphorus remaining in condensed phase. Approximately 30–35% of phosphorus is remaining in condensed phase for the three resins containing IL169. These calculations

Table 3
Main data from cone calorimeter tests (heat flux 35 kW/m^2).

Formulation	P content (wt%)	TTI (s)	pHRR (kW/m^2)	THR (kJ/g)	Residue (wt%)	EHC (kJ/g)	SEA (m^2/kg)
0IL	0	105	1099	23.7	2.5	24.3	810
10IL	1.45	96	629	16.2	15.1	19.1	1138
20IL	2.67	104	345	16.3	23.8	21.6	949
30IL	3.69	102	300	12.7	39.0	20.9	946

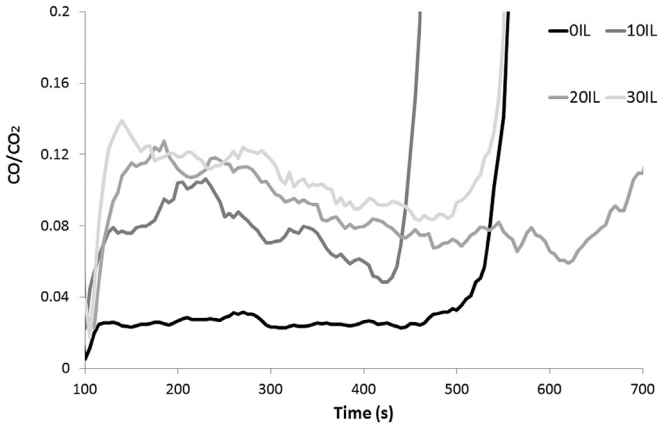

Fig. 8. CO/CO_2 ratio curves for the epoxy resins during cone calorimeter tests.

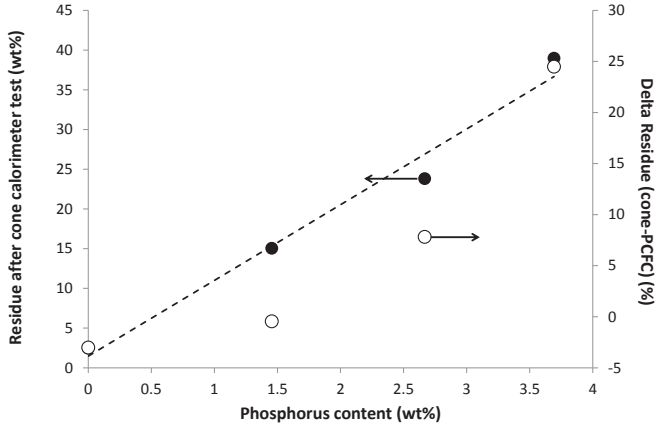

Fig. 9. Char content in cone calorimeter tests and difference between char contents in cone calorimeter and in PCFC versus phosphorus content in epoxy resins.

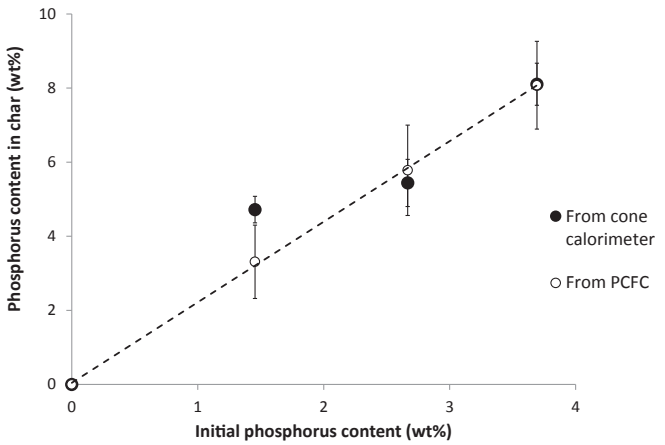

Fig. 10. Phosphorus content in char for residues sampled from cone calorimeter and PCFC tests.

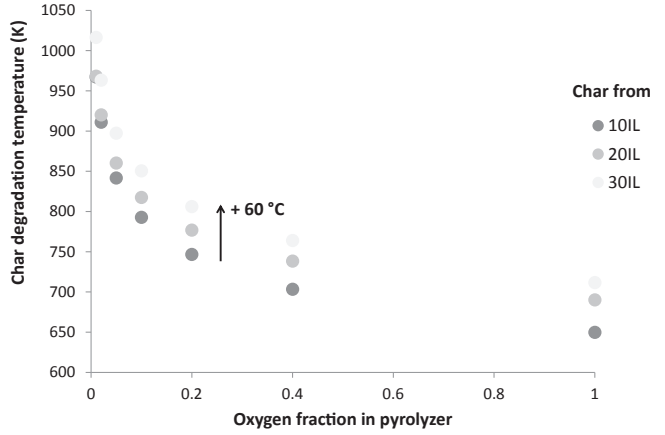

Fig. 11. Thermo-oxidative stability of chars from cone calorimeter tests.

show that more than 50 wt% of phosphorus is released in vapor phase. This is consistent with a possible flame inhibition effect of phosphorus.

Intumescence is a powerful strategy to reduce fire hazard. For example, intumescent coatings (including epoxy-based coating) are used to protect metallic structures. For such applications, the expanded char integrity must be maintained for a long time. If pyrolysis is believed to be anaerobic during flaming combustion, the char may undergo thermo-oxidation (i.e. aerobic pyrolysis) after flame out. The thermo-oxidative stability of chars sampled from cone calorimeter was assessed using PCFC by changing the oxygen fraction in pyrolyzer as recently proposed by Sonnier et al. [26].

As already mentioned, the residue from 0IL is not sampled from the core of the char and its composition is significantly different. Therefore the method was carried out only on the chars from IL-containing resins (Fig. 11). It appears clearly that the increase in phosphorus content leads to a higher thermo-oxidative stability. The temperature of char degradation increases from 10IL to 30IL whichever the oxygen fraction. The increase is about 60 °C at an oxygen fraction of 0.2.

It has already been proved that thermal stability is not only related to elemental composition but also to graphitization. The

Table 4
Elemental composition of chars.

Formulation	From cone calorimeter		
	C (wt%)	O (wt%)	P (wt%)
0IL	85.4	14.5	0
10IL	71.6	23.5	4.7
20IL	69	25.6	5.5
30IL	65.4	26.5	8.1

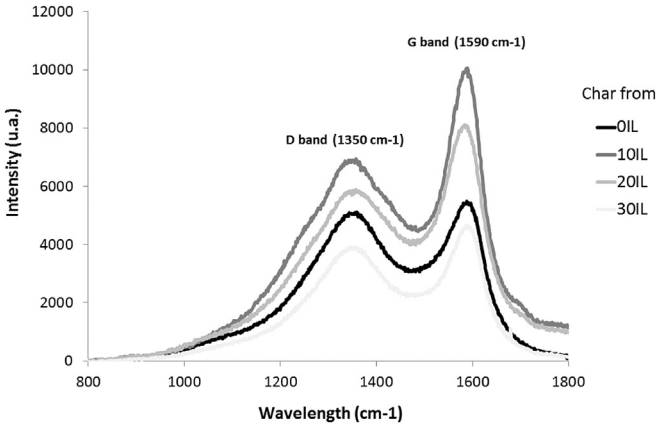

Fig. 12. Raman spectra of chars.

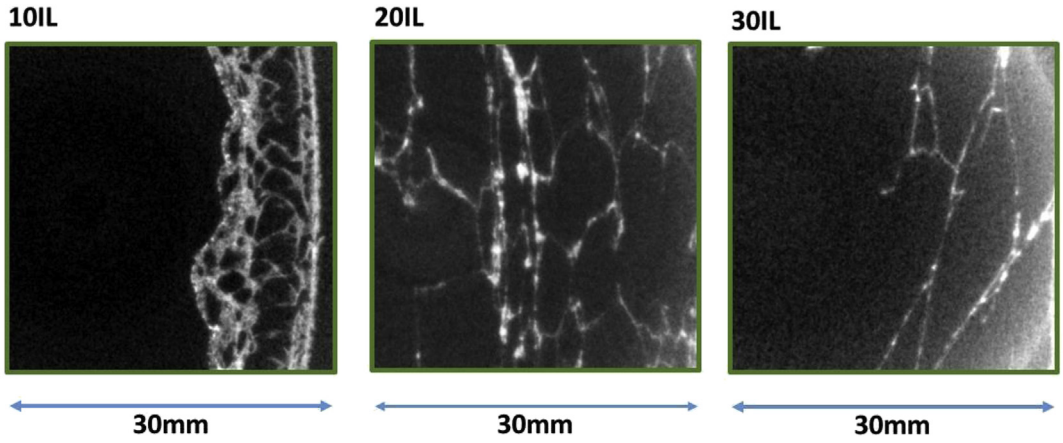

Fig. 13. X-ray microtomography images of chars from phosphorus-based epoxy resins.

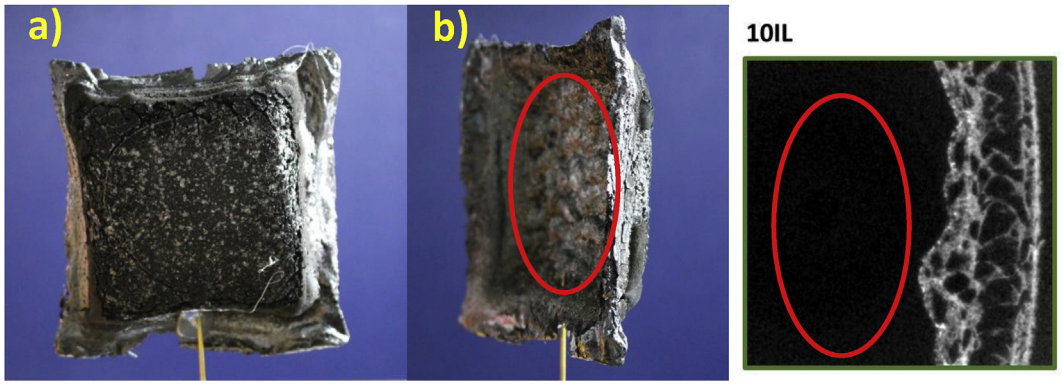

Fig. 14. Pictures of residues at the end of cone calorimeter test for 10IL sample, a) front side b) back view- Red ring corresponds to the hollow at back side of sample. (For interpretation of the references to colour in this figure legend, the reader is referred to the web version of this article.)

graphitization of char can be estimated by calculating the ratio between the integrated intensities of D and G bands on Raman spectra. According to the literature, D band corresponds to unorganized carbon structure. This band is related to the vibration of carbon atoms with dangling bonds in the plane terminations of disordered graphite or glass carbons. G band corresponds to an E2g mode of hexagonal graphite and is related to the vibration of sp^2-bonds carbon atoms in graphite layers [30–32]. Therefore, when the ratio of integrated intensities (I_D/I_G) decreases, graphitization increases. All Raman spectra of chars (Fig. 12) showed the presence of the two bands i.e. D band (1350 cm^{-1}) and G band (1590 cm^{-1}). The integration of bands (using a Lorentzian fitted curve method) showed that I_D/I_G ratio is decreasing for the samples containing phosphorous (2.33, 2.17, 2.56, respectively for 10IL, 20IL and 30IL) compared to the sample without phosphorous (2.94). Thus, it can be assumed that the presence of phosphorous increases the graphitization of char. Nevertheless, the change is not monotonous when increasing phosphorous content. This point is still under investigation.

The efficiency of an expanded char as a barrier layer to heat and gases largely depends on its structure (porosity, density, cell size …). Therefore the expanded char layers from cone calorimeter residues were studied using X-ray microtomography. The thickness of chars increased from 10IL to 30IL, as explained earlier (Fig. 7 – Residues in cone calorimeter), and a closed surface is observed in all cases, but the inner structure also changes to a large extent. Fig. 13 displays the pictures obtained from this measurement for 10IL, 20IL and 30IL samples. Open pores are observed particularly for 20IL and 30IL. The size of cells increases with increasing phosphorous percentage and is particularly high for the chars from 20IL and 30IL (several cm^3). There are more cells in the char from 10IL and the size of cells is smaller but the expansion is much more limited. Moreover, there is a hollow space on the back side of this char (Fig. 14).

4. Conclusions

Phosphorus-based ionic liquid is able to impart flame retardancy of epoxy networks wherein it is used initially as hardener. The peak of heat release rate and the total heat release in cone calorimeter decrease by 73% and 48% respectively in the presence of 30 phr of IL169, without reducing the time-to-ignition. Increasing incorporation of IL169 leads to increasing phosphorus content in char. Phosphorus improves the graphitization as well as the thermo-oxidative stability of the char. Expanded char allows protecting the underlying polymer even if its structure is not fully optimized.

Phosphorus modifies the decomposition pathway and promotes charring but may also act as flame inhibitor. It is interesting to note that both the cation and the anion of IL169 contain phosphorus. Different phosphorus moieties may act differently in condensed and gaseous phases in the studied materials.

Various ionic liquids containing phosphorus in different oxidation states or other flame retardant elements (as bromine or

chlorine) are available. They offer the possibility to finely tune the fire behavior of the epoxy networks through a reactive approach. Some of them are currently under investigation.

Appendix A. Supplementary data

Supplementary data related to this article can be found at http://dx.doi.org/10.1016/j.polymdegradstab.2016.10.009.

References

[1] S. Levchik, E. Weil, Thermal decomposition, combustion and flame-retardancy of epoxy resins - a review of the recent literature, Polym. Int. 53 (2004) 1901–1929.

[2] R.M. Perez, J.K.W. Sandler, V. Altstädt, T. Hoffmann, D. Pospiech, M. Ciesielski, M. Döring, U. Braun, U.I. Balabanovich, B. Schartel, Novel phosphorus-modified polysulfone as a combined flame retardant and toughness modifier for epoxy resins, Polymer 48 (2007) 778–790.

[3] B. Schartel, A.I. Balabanovich, U. Braun, U. Knoll, J. Artner, M. Ciesielski, M. Döring, R. Perez, J.K.W. Sandler, V. Altstädt, T. Hoffmann, D. Pospiech, Pyrolysis of epoxy resins and fire behavior of epoxy resin composites flame-retarded with 9,10-Dihydro-9-oxa-10-phosphaphenanthrene-10-oxide additives, J. Appl. Polym. Sci. 104 (2007) 2260–2269.

[4] T. Mariappan, Z. You, J. Hao, C. Wilkie, Influence of oxidation state of phosphorus on the thermal and flammability of polyuria and epoxy resin, Eur. Polym. J. 49 (2013) 3171–3180.

[5] P.M. Hergenrother, C.M. Thompson, J.G. Smith Jr., J.W. Connell, J.A. Hinkley, R.E. Lyon, R. Moulton, Flame retardant aircraft epoxy resins containing phosphorus, Polymer 46 (2005) 5012–5024.

[6] U. Braun, A.I. Balabanovich, B. Schartel, U. Knoll, J. Artner, M. Ciesielski, M. Döring, R. Perez, J.K.W. Sandler, V. Alstädt, T. Hoffman, D. Pospiech, Influence of the oxidation state of phosphorus on the decomposition and fire behaviour of flame-retarded epoxy resin composites, Polymer 47 (2006) 8495–8508.

[7] H. Ren, J. Sun, B. Wu, Q. Zhou, Synthesis and properties of a phosphorus-containing flame-retardant epoxy resin based on bis-phenoxy (3-hydroxy) phenyl phosphine oxide, Polym. Degrad. Stab. 92 (2007) 956–961.

[8] B. Schartel, U. Braun, A.I. Balabanovich, J. Artner, M. Ciesielski, M. Döring, R.M. Perez, J.K.W. Sandler, V. Altstädt, Pyrolysis and fire behavior of epoxy systems containing a novel 9,10-dihydro-9-oxa-10-phosphaphenanthrene-10-oxide-(DOPO)-based diamino hardener, Eur. Polym. J. 44 (2008) 704–715.

[9] C. Xie, B. Zeng, H. Gao, Y. Xu, W. Luo, X. Liu, L. Dai, Improving thermal and flame-retardant properties of epoxy resins by a novel reactive phosphorus-containing curing agent, Polym. Eng. Sci. 54 (2014) 1192–1200.

[10] G. Lligadas, J.C. Ronda, M. Galià, V. Cadiz, Development of novel phosphorus-containing epoxy resins from renewable resources, J. Polym. Sci. Part A: Polym. Chem. 44 (2006) 6717–6727.

[11] R. Menard, C. Negrell, L. Ferry, R. Sonnier, G. David, Synthesis of biobased phosphorus-containing flame retardants for epoxy thermosets: comparison of additive and reactive approaches, Polym. Degrad. Stab. 120 (2015) 300–312.

[12] B. Szolnoki, A. Toldy, P. Konrad, G. Szebeny, G. Marosi, Comparison of additive and reactive phosphorus-based flame retardants in epoxy resins, Period. Polytech. Chem. Eng. 57 (2013) 85–91.

[13] R. Menard, C. Negrell-Guirao, L. Ferry, R. Sonnier, G. David, Synthesis of biobased phosphate flame retardants, Pure Appl. Chem. 86 (2014) 1637–1650.

[14] R. Menard, C. Negrell, M. Fache, L. Ferry, R. Sonnier, G. David, From a bio-based phosphorus-containing epoxy monomer to fully bio-based flame retardant thermosets, RSC Adv. 5 (2015) 70856–70867.

[15] A. Silva, S. Livi, D. Netto, B. Soares, J. Duchet, J.-F. Gerard, New epoxy systems based on ionic liquid, Polymer 54 (2013) 2123–2129.

[16] S. Livi, A.A. Silva, Y. Thimont, B.G. Soares, T.K.L. Nguyen, J.F. Gérard, J. Duchet-Rumeau, Nanostructured thermosets from ionic liquid building block/epoxy prepolymer mixtures, RSC Adv. 4 (2014) 28099–28106.

[17] T.K.L. NGuyen, S. Livi, B.G. Soares, S. Pruvost, J. Duchet-Rumeau, J.-F. Gérard, Ionic liquids: a new route for the design of epoxy networks, ACS Sustain. Chem. Eng. 4 (2016) 481–490.

[18] T.K.L. NGuyen, S. Livi, S. Pruvost, J. Duchet-Rumeau, Bluma G. Soares, Ionic Liquids as reactive additives for the preparation and modification of epoxy networks, J. Polym. Sci. Part A: Polym. Chem. 52 (2014) 3463–3471.

[19] H. Maka, T. Spychaj, R. Pilawka, Epoxy resin/ionic liquid systems: the influence of imidazolium cation size and anion type on reactivity and thermo-mechanical properties, Ind. Eng. Chem. Res. 51 (2012) 5197–5206.

[20] H. Mąka, T. Spychaj, M. Zenker, High performance epoxy composites cured with ionic liquids, J. Ind. Eng. Chem. 31 (2015) 192–198.

[21] K.J. Fraser, D.R. MacFarlane, Phosphonium-based ionic liquids: an overview, Aust. J. Chem. 62 (2009) 309–321.

[22] A.-O. Diallo, A. Morgan, C. Len, G. Marlair, Revisiting physico-chemical hazards of ionic liquids, Sep. Purif. Technol. 97 (2012) 228–234.

[23] A.-O. Diallo, A. Morgan, C. Len, G. Marlair, An innovative experimental approach aiming to understand and quantify the actual fire hazards of ionic liquids, Energy & Environ. Sci. 6 (2013) 699–710.

[24] R.E. Lyon, R.N. Walters, Pyrolysis combustion flow calorimetry, J. Anal. Appl. Pyrolysis 71 (2004) 27–46.

[25] C. Huggett, Estimation of rate of heat release by means of oxygen-consumption measurements, Fire Mater. 4 (1980) 61–65.

[26] R. Sonnier, A. Viretto, B. Otazaghine, L. Dumazert, A. Evtsratov, J.-C. Roux, C. Heruijing, C. Presti, J. G. Alauzun, P. H. Mutin, H. Vahabi, Studying the thermo-oxidative stability of chars using pyrolysis-combustion flow calorimetry, Polymer Degradation and Stability, submitted.

[27] M. Muller, S. Bourbigot, S. Duquesne, R. Klein, G. Giannini, C. Lindsay, J. Vlaseenbroeck, Investigation of the synergy in intumescent polyurethane by 3D computed tomography, Polym. Degrad. Stab. 98 (2013) 1638–1647.

[28] P. Müller, M. Morys, A. Sut, C. Jäger, B. Illerhaus, B. Schartel, Melamine poly(zinc phosphate) as flame retardant in epoxy resin: decomposition pathways, molecular mechanisms and morphology of fire residues, Polym. Degrad. Stab. 130 (2016) 307–319.

[29] S. Brehme, B. Schartel, J. Goebbels, O. Fischer, D. Pospiech, Y. Bykov, M. Döring, Phosphorus polyester versus aluminium phosphinate in poly(butylene terephthalate) (PBT): flame retardancy performance and mechanisms, Polym. Degrad. Stab. 96 (2011) 875–884.

[30] X. Feng, W. Xing, L. Song, Y. Hu, In situ synthesis of a MoS2/CoOOH hybrid by a facile wet chemical method and the catalytic oxidation of CO in epoxy resin during decomposition, J. Mater. Chem. A 2 (2014) 13299–13308.

[31] A.M. Rao, E. Richter, S. Bandow, B. Chase, P.C. Eklund, K.A. Willams, S. Fang, K.R. Subbaswamy, M. Menon, A. Thess, R.E. Smalley, G. Dresselhaus, M.S. Dresselhaus, Diameter-selective Raman scattering from vibrational modes in carbon nanotubes, Science 275 (1997) 187–191.

[32] T. Tang, X. Chen, X. Meng, H. Chen, Y. Ding, Synthesis of multiwalled carbon nanotubes by catalytic combustion of polypropylene, Angew. Chem. 117 (2005) 1541–1544.